U.S. DEPARTMENT OF THE INTERIOR
U.S. GEOLOGICAL SURVEY

Prepared for the
NATIONAL AERONAUTICS AND SPACE ADMINISTRATION

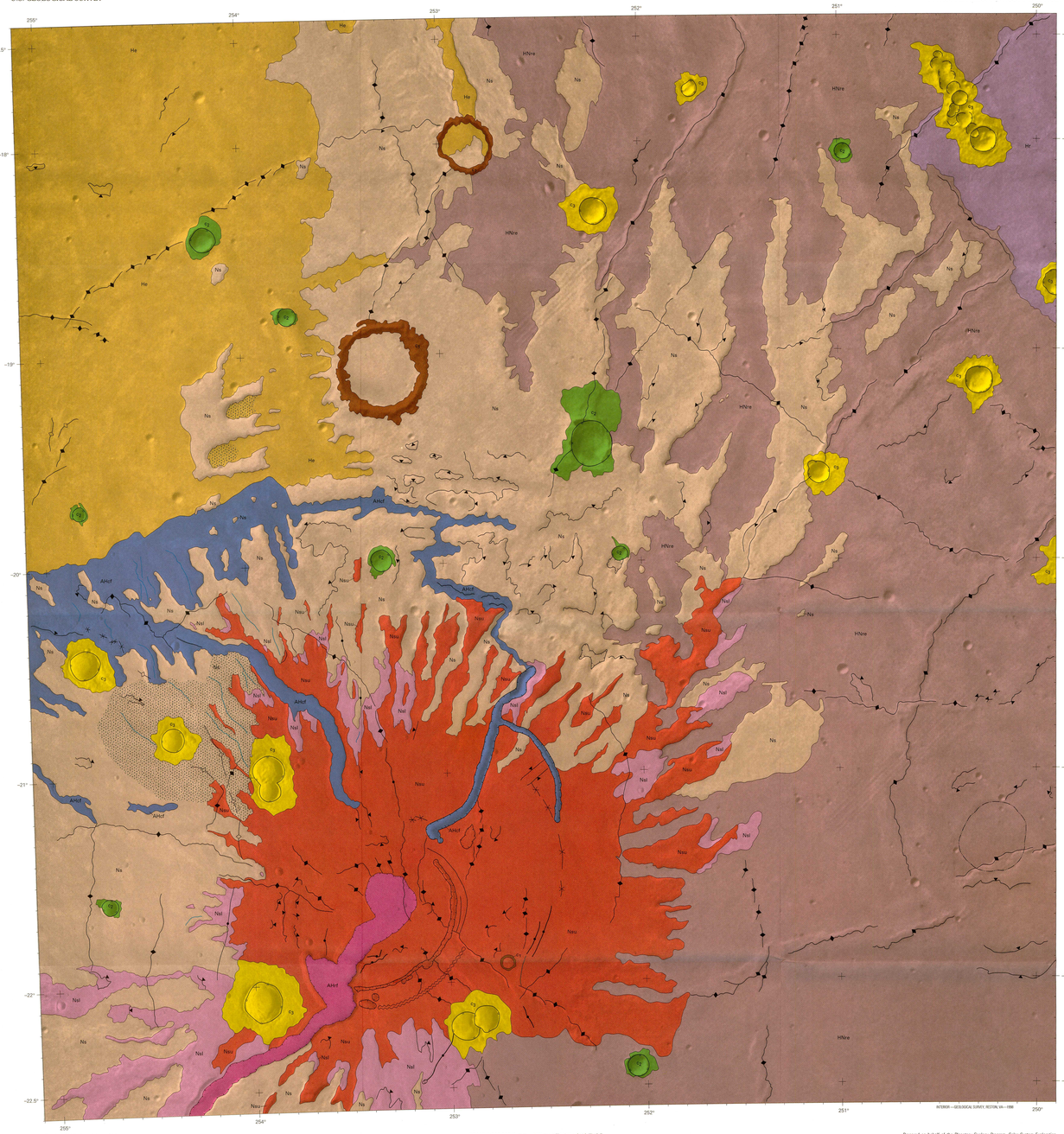

Base from U.S. Geological Survey, 1991.

SCALE 1:502 000 (1 mm = 502 m) AT 250° LONGITUDE
TRANSVERSE MERCATOR PROJECTION

10 0 10 20 30 40 50 60 70 80 90 100
KILOMETERS

INTERIOR—GEOLOGICAL SURVEY, RESTON, VA—1998

Prepared on behalf of the Planetary Geology Program, Solar System Exploration Division, Office of Space Science, National Aeronautics and Space Administration
Edited by Derrick D. Hirsch; cartography by Roger D. Carroll and Darlene A. Cavalier
Manuscript approved for publication June 26, 1995

CORRELATION OF MAP UNITS

SERIES	EROSIONAL MATERIALS	PLAINS MATERIALS	SHIELD MATERIALS	CRATER MATERIALS
AMAZONIAN	AHcf, AHrf		AHrf	c3, c2, c1
HESPERIAN		He, Hr, HNre		
NOACHIAN			Nsu, Nsl, Ns	

DESCRIPTION OF MAP UNITS

EROSIONAL MATERIAL

AHcf **Channel-floor material**—Mottled surface locally transected by narrow (<500 m), shallow, V-shaped channels. Locally within broad (~5 km wide), flat-floored, steep-walled channels dissecting shield materials. Observed only in high resolution (~50 m/pixel) Viking Orbiter images (VO445A series). *Interpretation:* Deposits composed of resorbed summit and basal shield material transported downslope by both fluvial and mass-wasting processes. Possible continuous around basal shield materials; resolution (~230 m/pixel; VO365S series) does not allow confirmation.

PLAINS MATERIALS

He **Etched plains material**—Broad, mottled plains with few mare-type ridges; shallow, capsate scarps observed parallel to and between ridges. Locally, scarps mantled with smooth deposits. Embays basal shield material west of Tyrrhena Patera summit. *Interpretation:* Precise origin unclear. Erosional scarps suggest nonresistant material such as thin lava flows or pyroclastic material. Smooth, mantling deposit may be reworked shield materials or etched plains material

Hr **Ridged plains material**—Broad, flat-lying plains with intersecting mare-type ridges typically oriented northeast or northwest; ridges oriented northwest crosscut ridges oriented northeast. Embays basal shield material northeast of Tyrrhena Patera summit, outside map area. *Interpretation:* Mare-type ridges suggest plains resulted from flood volcanism. Ridges may be caused by (1) local or regional tectonic deformation, (2) localized volcanic conduits, or (3) both volcanic and tectonic processes

HNre **Ridged and etched plains material**—Broad, mottled plains with intersecting mare-type ridges oriented northeast and northwest; areas between ridges locally exhibit shallow, fluted scarps. Embays shield materials north, east, and southeast of Tyrrhena Patera. *Interpretation:* Basal shield material mantled by younger deposit or less-resistant facies of ridged plains material or older, modified ridged plains material

SHIELD MATERIALS

AHrf **Rille-floor material**—Smooth, flat, featureless surface located within two elliptical depressions and connecting rille at Tyrrhena Patera summit; rille continues to southwest beyond map area and joins large (~1,000 km by ~200 km) field of flows and leveed channels, outside map area, which are elongate radial to summit. Rille crosses all shield materials; field of lobate scarps and leveed channels superposed on plains materials. *Interpretation:* Late-stage lava erupted from Tyrrhena Patera summit, forming floor of summit depressions and connecting rille

Nsu **Upper summit shield material**—Smooth (at ~50 m/pixel resolution) surface continuous on and around Tyrrhena Patera summit region; locally forms isolated mesas surrounded by basal shield and lower summit shield materials. Steep, theater-shaped scarps, typically directed away from summit region, define unit boundaries and form headwalls of broad (~5 km wide), flat-floored channels oriented radially to Tyrrhena Patera summit. Contains arcuate graben, crater chains, and short, narrow, arcuate ridges concentric to summit region, and short mare-type ridges radial to summit. High resolution (~11–13 m/pixel) Viking Orbiter images (79A001–12) reveal faint linear texture oriented west-northwest. Does not contain fully developed steep-walled, flat-floored channels. *Interpretation:* Pyroclastic deposits erupted from Tyrrhena Patera. Arcuate graben and pit-crater chains define collapse zone around summit caused by eruption or subsurface magma withdrawal. Narrow, concentric ridges interpreted as dikes exhumed by eolian removal of upper summit shield material

Nsl **Lower summit shield material**—Smooth to locally hummocky surface forms positive relief spurs and isolated, steep-sided mesas surrounded by basal shield material. Locally contains narrow (≤500 m wide), V-shaped, slightly sinuous channels. Discontinuous around upper summit shield material; greatest exposure in southern region of quadrangle. Steep to shallow scarps, typically directed away from summit region, define unit boundaries. *Interpretation:* Pyroclastic deposits erupted from Tyrrhena Patera. Scarp morphology and distribution indicative of modification by groundwater sapping

Ns **Basal shield material**—Smooth surface discontinuous around upper and lower summit shield materials up to ~200 km from summit region, and dissected by broad (~5 km wide), flat-floored channels. Forms floors of some broad channels and forms isolated, steep-sided mesas surrounded by channel floor material or embayed by plains materials. Steep scarps, typically directed away from summit region, define unit boundaries. Scarps locally exhibit two or more breaks in slope. *Interpretation:* Pyroclastic deposit erupted from Tyrrhena Patera. Morphology and distribution of scarps suggest modification by groundwater sapping processes. Breaks in slope observed on scarps may be separate cooling units, distinct volcanic events, or differential erosion of a single deposit

IMPACT CRATER MATERIALS

[Impact craters <3 km in diameter not mapped]

c3 **Well-preserved crater material**—Characterized by pronounced, continuous crater rim elevated relative to surrounding materials and by well-defined, continuous ejecta blanket. *Interpretation:* Pristine crater material with little degradation

c2 **Moderately degraded crater material**—Characterized by a crater rim that may exhibit only minor relief above surrounding materials and by discontinuous, poorly exposed ejecta. *Interpretation:* Impact craters having moderate age and degradation

c1 **Highly degraded crater material**—Degraded crater rim may be discontinuous and exhibits little relief relative to surrounding materials; no ejecta and smooth, featureless crater floors. *Interpretation:* Most degraded impact crater material. Ejecta has been completely eroded or mantled by younger materials; rim has been modified by erosion. Floors may be covered by mass-wasted, eolian or volcanic deposits

- **Contact**—Dashed where approximately located
- **Graben**
- **Mare-type wrinkle ridge**—Showing crest. Represents contact in places
- **Arcuate or linear ridge crest**—Represents contact in places
- **Ridge crest**—Possible dike
- **Scarp base**—Barb points downslope
- **Depression**
- **Narrow channel**
- **Pit-crater chain**
- **Crater rim**—Showing crest
- **Buried crater rim**—Showing crest
- **Mantling material**— Light-colored

INTRODUCTION

Mars Transverse Mercator (MTM) –20252 quadrangle contains the volcano Tyrrhena Patera, a low, broad structure that has summit depressions and is dissected by prominent radial channels (fig. 1). Tyrrhena Patera is surrounded by cratered plains materials on the western edge of Hesperia Planum, ~2,000 km northeast of the center of the Hellas basin (Greeley and Guest, 1987; U.S. Geological Survey, 1991). On the basis of Mariner 9 data, Tyrrhena Patera was interpreted to be a shield volcano, composed of fluid basic or ultrabasic lavas (Peterson, 1978; Pike, 1978). Analysis of Viking Orbiter images led Greeley and Spudis (1981) to suggest that Tyrrhena Patera comprises pyroclastic deposits produced by explosive hydromagmatic eruptions; Greeley and Crown (1990) support a pyroclastic origin for Tyrrhena Patera shield materials and assess several eruption styles for the volcano (see also Crown and Greeley, 1993). Summit-radial channels dissecting Tyrrhena Patera shield materials have theater-shaped heads, steep walls, and broad, flat floors; these morphologic characteristics are similar to those of terrestrial sapping channels (Greeley and Crown, 1990; Gulick and Baker, 1990; Crown and Greeley, 1993). Erosion of Tyrrhena Patera's shield materials by groundwater sapping is consistent with shield materials composed of friable deposits, such as pyroclastics. A volcano-tectonic rille extending from the summit of Tyrrhena Patera to the southwest crosscuts shield materials and joins a large (~1,000 km by ~200 km) field of lava flows southwest of the map area (Greeley and Crown, 1990; Crown and others, 1991), suggesting that Tyrrhena Patera may have experienced a transition from early explosive volcanism to late-stage effusive volcanism (Greeley and Spudis, 1981; Greeley and Crown, 1990). Morphology and relative ages of other Martian volcanoes suggest that the explosive-effusive transition observed at Tyrrhena Patera may reflect a similar global transition (Greeley and Spudis, 1981; Mouginis-Mark and others, 1988; Greeley and Crown, 1990; Crown and Greeley, 1993; Robinson and others, 1993). Previous attempts to constrain the timing of Tyrrhena Patera activity have resulted in a variety of reported ages for the shield materials. Pieri and Saunders (1979) counted the number of impact craters greater than 1 km in diameter on the Tyrrhena Patera shield materials and concluded that these shield materials were formed during the Noachian. Greeley and Guest (1987) show that Tyrrhena Patera shield materials are younger than the surrounding Hesperian-aged plains of Hesperia Planum and include the large southwest-flank flow field within Hesperia Planum. In contrast, Greeley and Crown (1990) rely on stratigraphic interpretations based on Viking Orbiter image analyses that indicate the shield materials are older than the surrounding Hesperian-aged plains but are also Hesperian in age. Detailed geologic study of Tyrrhena Patera and its stratigraphic relations with surrounding plains materials constrain the origin of the dissected shield materials, the degradational history at Tyrrhena Patera and the timing of volcanic activity within the southern cratered highlands of Mars.

GEOLOGY AND PHYSIOGRAPHIC SETTING

Highland materials (unit Npld of Greeley and Guest [1987]) east to the northwest, west, and southwest of MTM –20252 quadrangle and are embayed by a low flow field associated with Tyrrhena Patera and by plains materials; these relations indicate that Tyrrhena Patera was constructed on top of ancient highland materials (Greeley and Guest, 1987; Greeley and Crown, 1990; Crown and others, 1992).

The Tyrrhena Patera summit region includes a central caldera complex, which contains two elliptical depressions, surrounded by dissected shield materials of the volcano. The volcano-tectonic rille intersecting the summit depressions extends outside the map area to the southwest, where it joins a field of lava flow lobes. This lava flow field extends ~1,000 km to the southwest, where it is cut by Dao Vallis adjacent to the flanks of Hadriaca Patera (Crown and others, 1992; Crown and Greeley, 1993). The flow field crosscuts the plains materials, which surround and embay the volcano on all sides.

The volcano-tectonic rille, which joins the Tyrrhena Patera summit to the large southwest flow field, is aligned radial to Hellas, as is a rille-like channel on the volcano's northwest flank. Intersecting wrinkle ridges within the plains materials (and within the southwest lava flow field, outside the map area) are oriented radial and concentric to Hellas (Watters and Chadwick, 1989; Greeley and Crown, 1990; Porter and others, 1991), and the concentric ridges appear to be younger than the radial ridges (Porter and others, 1991). These structures suggest that the formation and evolution of the Hellas basin has exerted structural control within the map area throughout recorded geologic history. Concentric graben and a pit-crater chain at the Tyrrhena Patera summit are probably related to caldera formation; concentric valleys in the shield materials ~120 km north of Tyrrhena Patera also appear to be related to the evolution of the volcano.

STRATIGRAPHY

SHIELD MATERIALS

The oldest units within the map area are shield materials associated with Tyrrhena Patera. These materials are divided into basal shield material (unit Ns), lower summit shield material (unit Nsl), and upper summit shield material (unit Nsu). The basal shield material (unit Hbe of Greeley and Crown, 1990) crops out as far as ~175 km from the Tyrrhena Patera summit region and is characterized by a smooth, gently undulating surface. Eroded plains material (unit He) embays basal shield material to the north and west. Basal shield material is heavily dissected by broad (as wide as ~5 km), flat-floored channels oriented radially to the summit and commonly forms isolated, steep-sided mesas embayed by plains materials. Boundaries of basal shield material are defined by steep scarps (as high as ~300 m, on the basis of shadow measurements performed on Viking Orbiter images), which typically face away from the summit region. Locally, these scarps exhibit two or more cliffs separated by small breaks in slope, giving the scarps a stair-step appearance (fig. 2). The erosional morphology of the scarps and lack of primary flow features within basal shield material are consistent with a basal shield composed of friable materials, such as pyroclastic deposits (Greeley and Crown, 1990; Crown and others, 1992). Therefore, the observed layers in the basal shield materials may be caused by welding and compaction of ash flow tuffs (Sheridan and Ragan, 1976). Analogy with terrestrial pyroclastic deposits suggests that the layers may be composed of single, thick flows or of multiple, thinner flow units that cooled together (Crown and Greeley, 1993).

Lower summit shield material is morphologically similar to basal shield material but is stratigraphically younger and crops out discontinuously up to ~75 km from the Tyrrhena summit region. It is characterized by a mottled, locally hummocky surface bounded by steep scarps. Most of the broad, flat-floored channels, which dissect basal shield material, extend headward to dissect lower summit shield material as well. Similar to basal shield material, lower summit shield material lacks primary flow features and displays a morphology consistent with friable materials, such as pyroclastic deposits.

Upper summit shield material caps other shield materials and encircles rille-floor material (unit AHrf) at the summit of Tyrrhena Patera. Unit Nsu is bounded by steep scarps that typically are directed away from the summit region. The surface of upper summit shield material is smooth at ~50 m/pixel resolution (Viking Orbiter images, 445A series) and contains arcuate graben and pit-crater chains concentric to the summit, as well as small, mare-type wrinkle ridges radial to the northern summit depression. High resolution (~11–13 m/pixel Viking Orbiter images (79A001–12) of the summit region reveal narrow (<100 m), discontinuous, parallel ridges and grooves oriented west-northwest, aligned with the inferred strongest seasonal winds in the area (Greeley and others, 1993) (fig. 3). This suggests that upper summit shield material was or is being modified by eolian processes (Crown and Greeley, 1993). Small crater rims are obscured, and an incipient channel is observed within upper summit shield material (fig. 3); both observations indicate an erosional surface. Furthermore, the margins of upper shield material are arcuate and appear to be erosional, unlike the bulbous margins of lava flows. There is no evidence of primary flow features at any available resolution within the summit shield material. The eroded appearance and lack of flow features are consistent with upper summit shield material being composed of pyroclastic deposits.

Rille-floor material (AHrf) covers the floors of the rille connecting two elliptical depressions at the caldera summit and the depressions. Photoclinometric studies (Zisk and others, 1992) show that the maximum height of the depression walls is 470±50 m. The rille continues to the southwest, beyond the map area, where it joins a vast field of lava flows (~1,000 km by ~200 km) containing leveed channels, lobate flows, and two orthogonal sets of mare-type wrinkle ridges (Greeley and Crown, 1990; Crown and others, 1991; Porter and others, 1991). Rille-floor material and the associated lava flows crosscut all shield materials and are superposed on etched plains, ridged plains, and ridged and etched plains materials outside the map area, making rille-floor material the youngest material associated with Tyrrhena Patera. Rille-floor material is characterized by a smooth, flat, featureless surface. No primary flow structures are observed within the summit depressions and the rille floor; however, rille-floor material does not have the etched, erosional appearance of the shield materials. Association of rille-floor material with lava flows southwest of the summit indicates that rille-floor material is probably composed of ponded, late-stage lavas emplaced by eruptions within the summit caldera complex.

PLAINS MATERIALS

Three plains materials are contained within the map area: ridged and etched plains material (unit HNre), ridged plains material (unit Hr), and etched plains material (unit He). Ridged and etched plains material embays Tyrrhena Patera shield materials to the north, east, and south (outside the map area). Ridged and etched plains material is characterized by a broad, apparently flat-lying surface with fewer intersecting mare-type ridges than are typically observed in ridged plains material. Locally, within and outside the mapped region, areas between ridges exhibit shallow, fluted scarps. These scarps are morphologically similar to those within etched plains and shield materials and are interpreted to be erosional features. Scarps within ridged and etched plains material do not exhibit as much relief as, nor are as well defined, as those within etched plains material. Ridged and etched plains material may be a less-resistant facies of ridged plains material, and the observed scarps may be caused by preferential erosion of a less-coherent material. Alternatively, ridged and etched plains material may be basal shield material that has been mantled, and the mantle has subsequently experienced modification. It is also possible that ridged and etched plains material is compositionally distinct from ridged plains material and Tyrrhena Patera materials but has been deformed by the same processes that deformed ridged plains material. Because the contacts between etched plains, ridged and etched plains, and ridged plains materials are gradational, it is difficult to accurately interpret the mode of formation on the basis of morphology. However, crater statistics suggest that ridged and etched plains material is intermediate in age between shield materials and other plains materials (fig. 5; table 1), suggesting that ridged and etched plains material is basal shield material that has been thinly mantled by a younger deposit.

Ridged plains material (unit Hr of Greeley and Guest [1987]; unit Hrp of Greeley and Crown [1990]) embays basal shield material to the northeast of Tyrrhena Patera. It is characterized by a broad, relatively flat surface containing intersecting arcuate to sinuous mare-type wrinkle ridges. Within, and adjacent to, the map area, wrinkle ridges primarily trend northeast and northwest—approximately radial and concentric, respectively, to the Hellas basin (Watters, 1988; Watters and Chadwick, 1989; Porter and others, 1991; Crown and Greeley, 1993). On the basis of morphologic similarities between Martian ridged plains and the lunar maria, ridged plains material is interpreted to be composed of compressionally deformed shoreline lava flows (Carr, 1973; Greeley and Guest, 1987; Watters, 1988).

Etched plains material (unit He of Greeley and Crown [1990]) is characterized by a flat to undulating, slightly mottled surface containing few mare-type wrinkle ridges. This unit extends as far as ~700 km west and north of Tyrrhena Patera and embays Tyrrhena Patera shield materials to the northwest and west. Etched plains material exhibits scarps that are not as high as (on the basis of shadow measurements) nor as well defined as those bounding basal shield material. However, scarps within etched plains material have planforms similar to scarps bounding shield materials, suggesting that the scarps are erosional. A large volcano-tectonic rille on the northeast flank of Tyrrhena Patera grades into a sinuous channel, which crosscuts basal shield material and joins etched plains material. No primary flow features are observed within the rille, sinuous channel, or etched plains material.

Greeley and Crown (1990) proposed that etched plains material may be either a facies unit of ridged plains material or a pyroclastic deposit associated with Tyrrhena Patera. The spatial relation between the rille, channel, and etched plains material suggests that etched plains material adjacent to Tyrrhena Patera may be composed of lavas emplaced via this rille. However, lack of primary flow features, few mare-type wrinkle ridges (which are abundant in ridged plains material [Watters, 1988]), and morphologic similarity to basal shield material do not support the interpretation of etched plains material as composed of lava flows; if etched plains material is composed of lava flows, then the present surface is not primary. Etched plains materials likely does not represent a deposit from a gravity-driven pyroclastic flow originating at the summit of Tyrrhena Patera; crater statistics (see section titled "Impact Crater Statistics") indicate that etched plains material is younger than shield materials, which do not bear evidence of extensive late-stage mantling. Thus, although the origin of etched plains material remains unclear, it appears to have a complex history. Material was deposited and then eroded by mass wasting or fluvial processes to produce scarps.

EROSIONAL MATERIALS

Channel-floor material (unit AHcf) lies within the broad (as wide as ~5 km), flat-floored channels dissecting the shield materials and at the bases of scarps bounding the shield materials. Channel-floor material also exists within a volcano-tectonic rille, emanating north-northwest from the summit region. It is superposed on both plains materials and shield materials within the map area. Channel-floor material is characterized by a mottled, slightly hummocky surface containing small channels <500 m wide with "V"-shaped cross sections. These narrow channels are observed only in high resolution (~40–60 m/pixel Viking Orbiter images (445A22–26, 52–56) and are interpreted as secondary drainage features (Crown and Greeley, 1993). Channel-floor material is interpreted as fluvial or mass-wasting deposits composed of shield materials removed from the shield walls and transported downslope. The channels containing channel-floor material are steep-walled with theater-shaped heads. High-resolution images (~40–60 m/pixel) show that the channel floors contain nested channels, which also have theater-shaped heads and flat floors and which widen downslope to become as broad as the channels in which they originate. The channels appear to have evolved through headward erosion, with channel widening by deflation and slumping of lower summit shield material (Crown and Greeley, 1993) (fig. 5). These morphologies are similar to those of terrestrial sapping channels (Higgins, 1984; Laity and Malin, 1985; Gulick and Baker, 1990). During the sapping process, groundwater discharge is concentrated at the head of the channel; as the aquifer releases water into the channel, the aquifer material is weakened, and the channel head collapses. Collapsed wall material is transported downslope by a combination of wet mass wasting and fluvial processes (Higgins, 1984; Gulick and Baker, 1990). Dissection of shield materials by sapping channels is consistent with shield materials composed of pyroclastic deposits (Greeley and Crown, 1990; Crown and Greeley, 1993).

Groundwater sapping may begin by exploiting pre-existing channels. Thus, although channels dissecting the flanks of Tyrrhena Patera appear to have been enlarged by groundwater sapping, the origin of the channels remains unclear (Crown and Greeley, 1993); the channels may be enlarged lava channels, valleys formed by volcanic density flows (Reimers and Komar, 1979), or surface runoff channels.

STRUCTURE

The Hellas basin is centered ~2,000 km southwest of Tyrrhena Patera. Peterson (1978) suggested that Tyrrhena Patera is on a rim of the Hellas basin. Tyrrhena Patera may lie at the intersection of Hellas-related fractures with rings of another basin in the region (Schultz, 1984; Schultz and Frey, 1990). Hadriaca and Tyrrhena Paterae are aligned radially to the center of Hellas (Peterson, 1978; Schultz, 1984), as are Dao and Harmakhis Valles (~1,000 km southwest of Tyrrhena Patera). Crown and others (1992) noted a structural fabric oriented radial to the basin center on the east rim of Hellas. The volcano-tectonic rille extending from the summit of Tyrrhena Patera and the lava flow field it joins are also oriented radially to the center of Hellas. Mare-type wrinkle ridges within the southwest lava flow field are oriented either northwest (approximately concentric to Hellas) or northeast (approximately radial to Hellas); wrinkle ridges within ridged plains material adjacent to Tyrrhena (outside the map area) are similarly aligned (Watters and Chadwick, 1989; Crown and others, 1991; Porter and others, 1991). Structures oriented radial or concentric to the Hellas basin are found in materials that range in age from Noachian to Amazonian, suggesting that the formation and evolution of Hellas basin has exerted structural control in the map area throughout recorded geologic history.

Most plains units in MTM –20252 quadrangle contain long (≤110 km), mare-type wrinkle ridges; many ridges are either radial or concentric to Hellas (Watters and Chadwick, 1989; Porter and others, 1991). Porter and others (1991) noted that Hellas-concentric ridges appear to crosscut Hellas-radial ridges within the large flow unit on the flank of Tyrrhena Patera, outside the map area. Ridges within the Tyrrhena Patera flow field that are oriented concentric to Hellas appear to post-date flow field emplacement, whereas Hellas-radial ridges appear to have formed contemporaneously with flow field emplacement (Porter and others, 1991). This relation suggests that the timing of the deformation events can be bracketed by flow field emplacement (see section titled "Impact Crater Statistics").

Other structures within the map area are oriented concentric to the summit region of Tyrrhena Patera, indicating the development of the volcano has exerted local structural control. Valleys within basal shield material, ~120 km north of the summit, are concentric to the summit of Tyrrhena Patera. Arcuate graben and a pit-crater chain encircle the summit depressions of the volcano. Short, arcuate ridges within upper shield material are oriented concentric to the summit, and similar ridges within basal shield material are oriented radial to the summit.

Narrow, linear to arcuate ridges found within upper summit shield material are concentric to the summit region and are arranged en echelon (fig. 6). Within basal shield material, a series of these en echelon narrow ridges are arranged radially to the summit (fig. 7). The ridges are interpreted to be exhumed dikes, possibly intruded during the emplacement of the large field of lava flows southwest of the quadrangle, and are now being exposed by removal of the relatively friable shield materials. Alternatively, the ridges may be spatter ramparts constructed around volcanic fissures, as suggested for similar features on Alba Patera (Cattermole, 1990).

Arcuate graben and pit-crater chains within upper summit shield material encircle the summit depressions of Tyrrhena Patera. These structures crosscut upper summit shield material and, thus, postdate emplacement of the shield materials. Scarps bounding the elliptical summit depressions crosscut the arcuate graben and pit-crater chains. Photoclinometric studies (Zisk and others, 1992) show that the summit area dips inward. These temporal and spatial relations suggest that emplacement of lavas forming the large flow unit southwest of the map area may have been related to the formation of the graben, chain craters, and summit depressions.

Dissection patterns in basal shield material, ~120 km north of the summit of Tyrrhena Patera, are embayed by ridged and etched plains material and are concentric to the summit region. These patterns are morphologically similar to the broad, flat-floored channels found on the flanks of Tyrrhena Patera, which are oriented radial to the summit region. They may have originally been faults or zones of weakness, resulting from volcanic loading, which have subsequently been exploited and enlarged by erosional processes.

IMPACT CRATER STATISTICS

Because relative ages of all units in the quadrangle are not clear based on photogeologic study, the number and size distribution of superposed impact craters were determined for each unit (for example, Hartmann and others, 1981; Tanaka, 1986). Crater size frequencies were recorded using a Zeiss TG23 Particle-Size Analyzer, which automatically bins the data (Greeley and Gault, 1970). The standard scale, which includes bins with central diameters between 1.25 and 26.83 mm, was used, and exponentially increasing bin sizes were selected. Due to inconsistencies in image resolution, data from the smallest bin (<1.29 mm, corresponding to <~0.7 km) were not included in any analysis. Geologic units were mapped on the photographic bases for six adjacent 1:500,000-scale MTM quadrangles [–20247, –20252, –20257, –25247, –25252, –25257]. The area of each unit was calculated to allow the crater frequencies to be normalized to 10^6 km^2, this facilitates comparison between units and comparison to the Martian time-stratigraphic series (Tanaka, 1986). The uncertainty in crater frequency was calculated as in previous studies (Crater Analysis Techniques Working Group, 1978; Chapman and others, 1989). The error equals $\pm (N^{1/2})/A \times 10^6$, in which N is the cumulative number of craters greater than or equal to a given diameter and A is the area of a given unit in square kilometers. Data are plotted as cumulative number of craters greater than or equal to a given diameter as a function of crater diameter (fig. 4).

Comparison of size-frequency distributions, particularly the number of craters per 10^6 km^2 that are greater than or equal to 2 km in diameter (N(2)) and 5 km in diameter (N(5)), allows the relative ages of the geologic units to be determined (Tanaka, 1986) (table 1). The number of craters greater than or equal to 16 km in diameter (N(16)) is not used, because there are not enough craters of this size within the counted areas to be statistically significant.

The crater statistics yield a range of possible time-stratigraphic determinations for each unit (Tanaka, 1986). For some materials, N(2) and N(5) statistics yield disparate ages, with N(2) statistics consistently indicating younger ages than N(5) statistics. These disparate ages may reflect the possible age range for a single unit (suggesting a long emplacement time), or they may indicate a resurfacing event which modified or obliterated smaller craters. Where N(2) and N(5) statistics yield disparate ages, preference is given to the age indicated by N(5) statistics, as the statistics for the smaller craters are more likely to be affected by resurfacing processes. Where relative ages determined from crater statistics and stratigraphy interpreted from Viking Orbiter image analyses conflict, preference is given to the chronostratigraphic series that supports the observed geologic stratigraphy.

On the basis of photogeologic interpretation, Greeley and Crown (1990) suggested that etched plains material may be a volcanic unit associated with Tyrrhena Patera and that it was emplaced before basal shield material. N(2) and N(5) values indicate that etched plains material is younger than Tyrrhena Patera shield materials, and, thus, does not represent an ancient Tyrrhena Patera deposit. Greeley and Guest (1987) included the large lava flow field southwest of the map area within ridged plains material of Hesperia Planum; crater statistics show that the flow field is much younger than Hesperia Planum and that the flow field may be as young as Middle Amazonian (Crown and others, 1992). N(2) and N(5) values for the three plains materials suggest that ridged and etched plains material is not a facies of ridged plains or etched plains materials. Instead, crater statistics indicate that ridged and etched plains material may be transitional in age between basal shield material and ridged plains material. The presence of fluted scarps within ridged and etched plains material suggests that the surface has been modified by erosional or depositional processes, or both. Crater statistics may not reflect the true age of ridged and etched plains material, but they may reflect a mixture of ages: the age of the original surface and the age(s) of subsequent modification(s).

By combining crater statistics for basal shield, lower summit shield, and upper summit shield materials, an average age for Tyrrhena Patera materials (including the much younger rille-floor material) can be estimated. The Tyrrhena Patera shield materials yield an average N(2) of 654±214 and N(5) of 440±179. These statistics suggest an age of Middle to Upper Noachian for the Tyrrhena Patera shield deposits (Tanaka, 1986), consistent with the age for Tyrrhena Patera determined by Plescia and Saunders (1979). Similarly, an average plains material age can be determined by combining the crater statistics for etched plains, ridged plains, and ridged and etched plains materials, giving an N(2) of 490±61 and an N(5) of 149±33. These statistics suggest an average age of Lower to Upper Hesperian for the plains materials adjacent to Tyrrhena Patera, consistent with the age of Martian ridged plains given by Plescia and Saunders (1979) and by Tanaka (1986).

GEOLOGIC HISTORY

The oldest units within MTM –20252 quadrangle are shield materials associated with Tyrrhena Patera. The erosional morphology of these materials is consistent with friable deposits, presumably pyroclastic, resulting from magma/groundwater interactions or from explosive release of magmatic volatiles (Greeley and Spudis, 1981; Greeley and Crown, 1990; Crown and Greeley, 1993). Channels formed on the flanks of Tyrrhena Patera after emplacement of shield materials; they may have initially been lava channels, valleys formed by volcanic density flows (Reimers and Komar, 1979), or surface runoff channels. These channels now have broad, flat floors with theater-shaped heads and appear to have been modified through groundwater sapping processes (Gulick and Baker, 1990; Crown and Greeley, 1993). The presence of mottled deposits, interpreted as alluvium, in the floors and at the mouths of these channels (superposed on plains materials) suggests that the channels have been active since emplacement of plains materials.

Plains materials (ridged plains, etched plains, and ridged and etched plains materials) embay Tyrrhena Patera shield materials on all sides of the volcano. Plains materials appear to have been emplaced at approximately the same time, and all may be facies of the same unit. Ridged plains material is interpreted as sheetlike lava flows; ridged and etched plains material is interpreted to be basal shield material mantled by a smooth deposit; and the origin of etched plains material is not clear, although it does not appear to be composed of lava flows and has been modified by erosion and subsequent mantling.

Rille-floor material and associated lava flows southwest of the map area erupted from Tyrrhena Patera after emplacement of the plains materials; this effusive activity may have continued into the Lower Amazonian (Crown and others, 1992). Narrow, arcuate ridges, interpreted as dikes, may have been intruded contemporaneously with rille-floor material, although they could have been intruded any time subsequent to emplacement of the shield materials. Mare-type ridges oriented northeast (radial to Hellas) were formed during the emplacement of the southwest lava flow field and are possibly related to lava effusion or sub-surface lava transport (Porter and others, 1991). Elliptical depressions, concentric graben, and a pit-crater chain at the summit of Tyrrhena Patera may be related to magma withdrawal through emplacement of the large lava flow field.

Following the formation of northeast-trending ridges, emplacement of the southwest lava flow field caused, and mare-type ridges oriented northwest (concentric to Hellas) formed by compression. Erosion continued to modify Tyrrhena Patera, both by wind—suggested by the faint linear texture observed at the summit—and by transport of material downslope within the broad channels radiating from the summit.

REFERENCES

Carr, M.H., 1973, Volcanism on Mars: Journal of Geophysical Research, v. 78, no. 20, p. 4049–4062.

Cattermole, Peter, 1990, Volcanic flow development at Alba Patera, Mars, Icarus, v. 83, p. 453–493.

Chapman, M.G., Masursky, Harold, and Dial, A.L., 1989, Geologic maps of science study site 1A, East Margaritifer Vallis, Mars: U. S. Geologic Survey Miscellaneous Investigations Series Map I–1962, scale 1:500,000.

Crater Analysis Techniques Working Group, 1978, Standard techniques for presentation and analysis of crater size-frequency data: National Aeronautics and Space Administration Technical Memorandum 79730.

Crown, D.A. and Ronald Greeley, 1993, Volcanic geology of Hadriaca Patera and the eastern Hellas region of Mars: Journal of Geophysical Research, v. 98, no. E2, p. 3431–3451.

Crown, D.A., Porter, T.K., and Greeley, Ronald, 1991, Physical properties of lava flows on the southwest flank of Tyrrhena Patera, Mars, in Abstracts of papers submitted to the 22nd Lunar and Planetary Science Conference, LPI, Houston, p. 261–262.

Crown, D.A, Price, K.T. and Greeley, Ronald, 1992, Geologic evolution of the east rim of the Hellas basin, Mars: Icarus, v. 100, p. 1–25.

Greeley, Ronald, and Crown, D.A., 1990, Volcanic geology of Tyrrhena Patera, Mars: Journal of Geophysical Research, v. 95, no. B5, p. 7133–7149.

Greeley, Ronald, and Gault, D.E., 1970, Precision size-frequency distributions of craters for 12 selected areas of the lunar surface: Moon, v. 2, p. 10–77.

Greeley, Ronald, and Guest, J.E., 1987, Geologic map of the eastern equatorial region of Mars: U.S. Geological Survey Miscellaneous Investigations Series Map I–1802–B, scale 1:15,000,000.

Greeley, Ronald, Skypeck, Andrew, and Pollack, J.B., 1993, Martian aeolian features and deposits: Comparisons with general circulation model results: Journal of Geophysical Research, v. 98, no. E2, p. 3183–3196.

Greeley, Ronald, and Spudis, P.D., 1981, Volcanism on Mars: Reviews of Geophysics and Space Physics, v. 19, no. 1, p. 13–41.

Gulick, V.C., and Baker, V.R., 1990, Origin and evolution of valleys on Martian volcanoes, Journal of Geophysical Research: v. 95, no. B9, p. 14,325–14,344.

Hartmann, W.K., Strom, R.G., Weidenschilling, S.J., Blasius, K.R., Chapman, C.R., Shoemaker, E.M., and Jones, K.L., 1981, Chronology of planetary volcanism by comparative studies of planetary cratering, *in* Basaltic volcanism on the terrestrial planets, Basaltic Volcanism Study Project, Pergamon, p. 1049–1127.

Higgins, C.G., 1984, Piping and sapping: Development of landforms by groundwater outflow, *in* Groundwater as a geomorphic agent, R.G. LaFleur, ed., Boston, Allen and Unwin, p. 18–58.

Laity, J.E., and Malin, M.C., 1985, Sapping processes and the development of theater-headed valley networks on the Colorado Plateau: Bulletin of the Geological Society of America, v. 96, p. 203–217.

Mouginis-Mark, P.J., Wilson, Lionel, and Zimbelman, J.R., 1988, Polygenic eruptions on Alba Patera, Mars: Bulletin of Volcanology, v. 50, p. 361–379.

Peterson, J.E., 1978, Volcanism in the Noachis-Hellas region of Mars, 2, in Lunar and Planetary Science conference, 9th, Houston, March 13–17, 1978, Proceedings: Lunar and Planetary Institute, Houston, p. 3411–3432.

Pike, R.J., 1978, Volcanoes on the inner planets: Some preliminary comparisons of gross topography, *in* Lunar and Planetary Science Conference, 9th, Houston, March 13–17, 1978, Proceedings: Lunar and Planetary Institute, Houston, p.3239–3273.

Plescia, J.B., and Saunders, R.S., 1979, The chronology of Martian volcanoes, *in* Lunar and Planetary Science Conference, 10th, Houston, March 14–18,1979, Proceedings: Lunar and Planetary Institute, Houston, p. 2841–2859.

Porter, T.K., Crown, D.A., and Greeley, Ronald, 1991, Timing and formation of wrinkle ridges in the Tyrrhena Patera region of Mars, in Abstracts of papers submitted to the 22nd Lunar and Planetary Science Conference, LPI, Houston, p. 1085–1086.

Reimers, P.E., and Komar, P.D., 1979, Evidence for explosive volcanic density currents on certain Martian volcanoes: Icarus, v. 39, p. 88–110.

Robinson, M.S., Mouginis-Mark, P.J., Zimbelman, J.R., Wu, S.S.C., Ablin, K.K., and Howington-Kraus, Anne, 1993, Chronology, eruption duration, and atmospheric contribution of the Martian volcano Apollinaris Patera: Icarus, v. 104, p. 301–323.

Schultz, P.H., 1984, Impact basin control of volcanic and tectonic provinces on Mars, *in* Abstracts of papers submitted to the 15th Lunar and Planetary Science Conference, LPI, Houston, p. 728–729.

Schultz, R.A., and Frey, H.V., 1990, A new survey of multiring impact basins on Mars: Journal of Geophysical Research, v. 95, no. B9, p. 14,175–14,189.

Sheridan, M.F., and Ragan, D.M., 1976, Composition of ash-flow tuffs, *in* Compaction of coarse-grained sediments, II, Developments Sedimentology, v. 18B